Journal of Hydrology 534 (2016) 317–325

Contents lists available at ScienceDirect

Journal of Hydrology

journal homepage: www.elsevier.com/locate/jhydrol

Coupling catchment hydrology and transient storage to model the fate of solutes during low-flow conditions of an upland river

D. Trévisan [a,*], R. Periáñez [b]

[a] INRA Carrtel, 75 avenue de Corzent, BP 511 74203 Thonon les Bains, France
[b] Departamento Fisica Aplicada I, ETSIA, Universidad de Sevilla, Ctra. Utrera km. 1, 41014 Sevilla, Spain

ARTICLE INFO

Article history:
Received 17 October 2014
Received in revised form 10 July 2015
Accepted 29 December 2015
Available online 8 January 2016
This manuscript was handled by Laurent Charlet, Editor-in-Chief, with the assistance of Antonio Lo Porto, Associate Editor

Keywords:
Transient storage
OTIS
Rhodamine WT
Hyporheic zone
Channel storage
Headwaters

SUMMARY

The residence time of solutes in catchments is longer during low-flow conditions, due to the lengthening of transport routes and the decrease in transfer velocities. In rivers, transient storage depends largely on exchanges with channel storage and the hyporheic zone and reflects the capacity of the river to buffer pollutant loads before they enter the aquatic environment of final receptors. Our objective was to evaluate the fate of solutes along a typical confined river of upland catchments. First, we calculate lateral inflows using a variable-source hydrology approach. Then, water motion and quality in the river channel are predicted by combining hydrodynamics and exchanges with channel storage and the hyporheic zone. The model is mainly parametrized from literature data during baseflow conditions to mimic the fate of adsorptive and non-persistent pollutants. Residence time in surface water, channel storage and the hyporheic zone were found to be sensitive to lateral inflows from groundwater seepage. Channel storage is the main process controlling residence time in upstream conditions, where the riverbed is mainly composed of stones and bedrock. Downstream, along with the formation of sediment deposits and riffle-pool units, hyporheic exchanges also control the lag time in the transfer of solutes. By integrating physically-based processes, the number of parameters is small, but the model still requires a detailed description of stream geometry and morphology. It can be used to evaluate stream restoration or catchment-river management when detailed data of stream geometry and morphology are available.

1. Introduction

Many compounds, such as xenobiotics, heavy metals or nutrients, can be transported in solution, affecting the ecological state, quality and use of rivers and other surface waters (Tlili et al., 2008). For ecological and economic issues, evaluating the environmental fate of solutes in river ecosystems remains a challenge to the preservation and management of natural resources (Martin and McCutcheon, 1998). The behaviour of river ecosystems depends on sequential inflows of water from groundwater seepage or surface run-off (USAEWES, 1995; Trévisan et al., 2012). Low-flow conditions, corresponding to events during which water and solute flows depend only on groundwater seepage, are of particular importance, as residence time increased. For forested or grassland upland catchments, where soils are relatively shallow and overlie impervious substrata, groundwater seepage occurs in contributing areas located at the bottom of slopes or in the centre of thalwegs (Obled and Zin, 2004; Trévisan et al., 2010). These processes are described by the "variable-source hydrology" concept and are modelled by semi-distributed models, such as TOPMODEL (Beven and Kirkby, 1979), or fully distributed models, such as SMDR (Hively et al., 2006). Once chemicals have entered a hydrological network, their fate depends on their chemical properties, biochemical and biological interactions, and also transient storage. Transient storage of chemicals within a river channel is related to channel storage (CS), corresponding to transfer delays occurring in the surface water (SW) column due to eddies or dead water zones, and to exchanges with the hyporheic zone (HZ), a compartment such as sediments or bank material within which SW can infiltrate and move (Gooseff et al., 2005; Uijttewaal et al., 2001). In headwaters, major representative river features, such as colluvial, step-pool and riffle-pool channel types, have been identified by Hassan et al. (2005) and Chin and Wohl (2005). They have been associated with specific transient exchange patterns (Buffington and Tonina, 2009).

Considering the role transient storage plays in the river buffering effect, more information about transient storage is necessary to quantify, control and manage pollution, and to better recognise where transient storage occurs in stream. Transient storage has

* Corresponding author.
E-mail address: dominique.trevisan@thonon.inra.fr (D. Trévisan).

http://dx.doi.org/10.1016/j.jhydrol.2015.12.058
0022-1694/

been the subject of many modelling studies. Water exchanges within gravel beds have been simulated in laboratory conditions (Tonina and Buffington, 2007; Cardenas and Wilson, 2007), coupling the St. Venant equation and Darcy's law to predict hyporheic residence time. Under field conditions, given the inherent variability of hydraulic properties and exchange rates along rivers and their alluvial deposits, models consider advection–diffusion in the SW and a source-sink term -a kernel- to account for transient storage. The kernel estimates a density of mass-transfer rate within transient stores, often with an exponential or power-law distribution (Haggerty et al., 2002; Gooseff et al., 2005, 2006). Transient-storage equations with exponential laws represent a typical case modelled by the One-Dimensional Transport with Inflow and Storage model (OTIS), which was developed to analyse feedback between SW and groundwater (Bencala and Walters, 1983; Herrman et al., 2010), the effect of flow obstruction on transient storage (Stofleth et al., 2008) or the fate of nitrogen along a river network (Stewart et al., 2011). Neilson et al. (2010) and Briggs et al. (2009) improved OTIS equations, separating transient storage into surface (dead zones) and HZ components. Whilst there is a consistent body of studies concerning processes occurring within rivers, sediments and aquifers, models of transient storage mainly have site-specific parameters or concern short river reaches. They do not help for regional scale analysis – notably several-km-long rivers – of relations between catchment and river morphology and their consequences on water flows and transient storage of solutes (Environment Agency, 2009).

To contribute to this topic, we applied a one-dimensional transport model that considers morphological and hydrodynamic descriptors, to couple water inputs from groundwater seepage, and the transport of solutes in a river system during low-flow conditions. Model predictions were compared to breakthrough curves (BTC) recorded at two locations downstream of the injection point of a non-persistent-reactive dye (Rhodamine WT, or RWT). Sensitivity analysis was performed to study relations between catchment and river features and the residence time of solutes in SW, CS and HZ.

2. Site and methods

2.1. Site

The Gordes River catchment (10 km^2) is representative of upland rivers of the southern shore and foothills of the Lake Léman basin in France (Fig. 1). The head of the catchment is located in calcareous sedimentary formations. On the upper part of the catchment (upstream of point A, Fig. 1), where the substratum consists of shales and sandstones, slopes are steep (mean 25–30%) and dominated by forests. Calcareous moraines are well represented in the foothills in the centre of the catchment (from A to C, Fig. 1), associated with a gently rolling landscape, where slopes range from 10% to 15%. Here grasslands and annual crops dominate, with scattered spots of urban development. The flat lower and morainic part (0.5–5%) of the basin is mainly covered by forests, whereas urban areas increase near the lake shore. The soils developed on the upper part are mainly Haplic Cambisols (brownish discolouration and structure formation in the soil profile, with no particular soil features). Those on moraine areas are Eutric Cambisols (base saturation of 50–70% from 20 to 100 cm) (World Reference Base for Soil Resources, 2006).

The river studied (7 km long) drains the entire sequence of forest – agricultural land – forest (Fig. 1). From points A to C, the depth and width of the riverbed were recorded every 10–20 m. We used a GPS (MobileMapper-Magellan) to reference the geographic coordinates of recorded data. The high of river banks, river width and depth were evaluated from direct or trigonometric measurements by means of a clinometer, a decameter and a tape fixed on a stick. Field data were interpolated using a geographic information system (Quantum GIS) to map the river bottom and define a 1D computational domain consisting of a succession of cells 1 m long, each associated with a rectangular section of defined width and surface area. Mean diameter of gravels, stones, and boulders and mean texture of bed sediments were also recorded, as was the presence of woody debris and the overall configuration of riverbed morphology (width, depth, presence of riffle, pools, etc.). Approximately 500 m downstream of point B (Fig. 1), a first-order tributary reaches the studied river, causing a net increase in river flow. According to Buffington and Tonina (2009), reach A–B (mean slope: 3.6%) belongs to the "bedrock" type, in which mainly pebbles (5–20 cm diameter) and sometimes boulders (>40 cm) cover the riverbed. This reach also has short passages of riffle and step-pool channel types, in which fine sediments can be observed in flow paths with lower velocity. These features were systematically described, their length, width and geographical location where measured and recorded. Reach B–C (mean slope 1.9%) meanders somewhat and mainly corresponds to a succession of confined riffles from alluvial deposits and step-pool features. Along this lower part of the river, depth and width increase. Sediments mainly consist of gravels in riffles preceding step-pools and of fine sandy material in pools. The mean distance between pools is about 5–10 m. The studied river has about 85% of its morphological features associated with colluvial and alluvial fill. Each cell of the computational domain was assigned to bedrock, riffle or pool, which meant that its HZ was assigned to stone, gravel or fine sediment, respectively.

2.2. Dye injection

To mimic in-stream effects (degradation, retention-release) that commonly affect the fate of solutes, RWT was injected during low-flow conditions. Given its adsorptive and extinction behaviour, 46.76 g of RWT was injected in a single dose at point A (Fig. 1). Fluorescence was recorded at point B (1022 m down-slope of the injection point) for 5.5 h using a CGUN-FL fluorimeter. The probe was then moved to point C (4198 m down-slope of point B), and data recording continued for 24 h until noise was detected in the probe signal. Steady-state conditions for discharge were verified throughout the monitoring. Sodium chloride was also injected to measure local water discharges at points B and C, using a CS547A Campbell conductivity probe.

2.3. Model

2.3.1. River and transient storage

We considered both CS and HZ exchanges (Fig. 2). The river is composed of a succession of one-dimensional cells of length Δx (1 m), where exchanges of water and solutes take place between SW, CS and the HZ (underlain by an impervious layer).

Longitudinal water velocity u in the SW (m s^{-1}) is:

$$\frac{\partial u}{\partial t} = -u\frac{\partial u}{\partial x} - g\left(\frac{\partial \eta}{\partial x} + \frac{u|u|}{C^2 h}\right) \quad (1)$$

where t is time (s), $g = 9.81$ m s^{-2} is acceleration due to gravity, η is the height of the water surface-measured above a reference level (m), h is the depth of SW (m) and C is Chezy's friction coefficient ($m^{-1/2}$ s^{-1}). This is obtained from $C = \frac{1}{n}W_p^{1/6}$, where n is Manning's roughness coefficient ($m^{-1/3}$ s) and W_p is the hydraulic radius (m). Following Cardenas and Wilson (2007) and Tonina and Buffington (2007), longitudinal velocity u_z (m s^{-1}) in the HZ is obtained from Darcy's law:

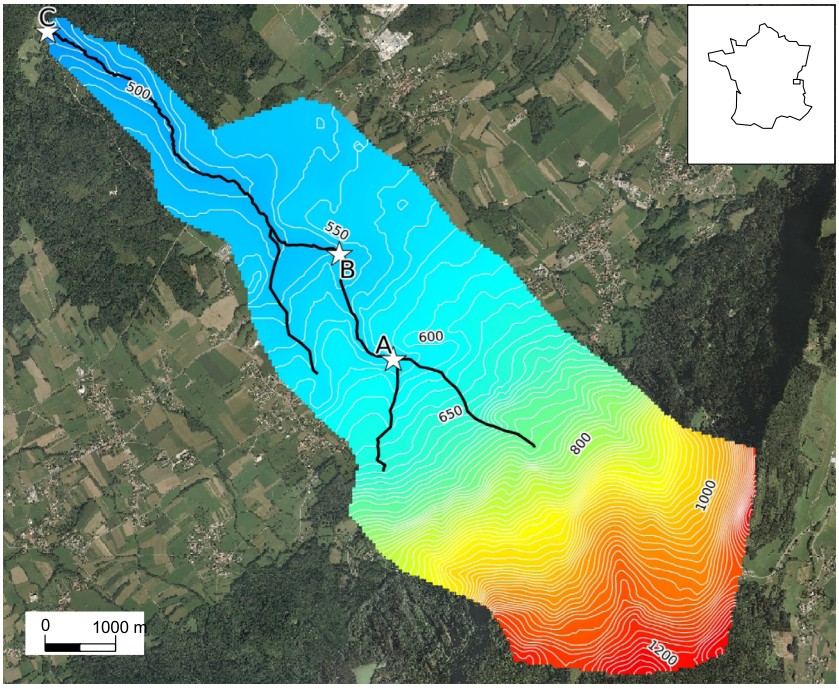

Fig. 1. The study catchment of the Gordes River, France. Isolines are in m.

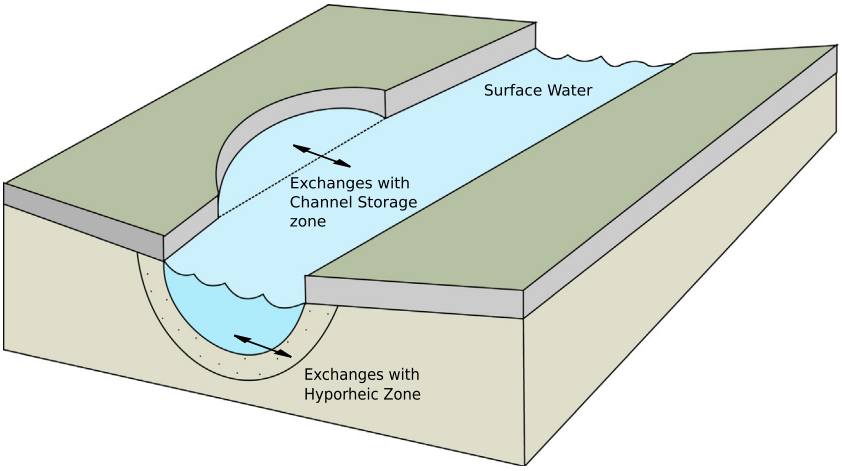

Fig. 2. Diagram of transient storage between surface water (SW), channel storage (CS) and hyporheic zones (HZ).

$$u_z = \frac{q_z}{A_z} = -K_z \frac{dH}{dx} \tag{2}$$

where q_z is longitudinal water flow along the HZ ($m^3\ s^{-1}$), A_z the area of the transverse section of the HZ (m^2), K_z the saturated hydraulic conductivity of the HZ ($m\ s^{-1}$) and H the total head (m), given by $dH = dh_0 + d\eta$, where h_0 is the elevation of the surface of the HZ above the reference level (m). The water flow r ($m^3\ s^{-1}$) between SW and the HZ is given by:

$$r = q_z(x) - q_z(x + \Delta x) \tag{3}$$

r having positive values when water flows from the HZ to SW and negative values when it flows the opposite way. Eqs. (1) and (2) are linked through the continuity equation (Prandle, 1974; Baeza et al., 2006):

$$S\frac{\partial \eta}{\partial t} = -\Delta x \frac{\partial (A_w u)}{\partial x} + r + Q_L \tag{4}$$

where S is the horizontal surface area of a cell between adjacent sections (m^2), A_w is the area of the transverse section of SW (m^2) and Q_L is the lateral inflow from the catchment ($m^3\ s^{-1}$).

2.3.2. Lateral inflows from the catchment

In the morainic context of the basins studied, soils are shallow and developed from impervious bedrocks, and lateral inflows are mainly related to variable-source hydrology (Trévisan et al., 2010; Gerard-Marchant et al., 2006). In cell k and during low-flow conditions, the lateral inflow Q_{L_k} feeding the river corresponds to groundwater discharge. It was estimated from TOPMODEL equations (Beven and Kirkby, 1979; Obled and Zin, 2004):

$$Q_{L_k} = a_k K_0 M \exp\left(\frac{D}{M}\right) \exp(-\Lambda) \tag{5}$$

where a_k is the total area contributing to cell k (m^2), K_0 is saturated hydraulic conductivity of the upper soil level ($m\ s^{-1}$), M (dimen-

sionless) is a parameter representing the decrease in saturated hydraulic conductivity with soil depth, D is the soil saturation deficit (dimensionless) and Λ is the mean topographic index (dimensionless). This last parameter is obtained from $\Lambda = \frac{1}{A_m}\int \ln\left(\frac{a_k}{\mathrm{tg}\beta}\right) da_k$, where A_m is the catchment area (m^2) and β is the terrain slope angle (gr).

2.3.3. Solute concentration

The potential adsorption of RWT on the solid phase (Yellow Spring Instruments, 2001), as well as decay in SW induced by photolysis (Keefe et al., 2004), were considered. We defined C_w, C_c, C_i and C_s as the solute RWT concentrations ($g\,m^{-3}$) in SW, CS, the fluid phase and the solid phase of HZ, respectively. Sorption dynamics were successfully modelled by Postma and Appelo (2000), assuming a linear sorption isotherm: $C_s = K_d C_i$, where K_d is the sorption isotherm constant ($m^3\,g^{-1}$). Considering the dimensionless retardation factor $R = 1 + \frac{\rho_b}{\theta}K_d$, where ρ_b is bulk density ($g\,m^{-3}$) and θ is HZ porosity (dimensionless), RWT concentrations in SW, CS and the HZ fluid phase are given by:

$$\frac{\partial C_w A_w}{\partial t} = -\frac{\partial(uC_wA_w)}{\partial x} + \frac{D_w\partial^2(C_wA_w)}{\partial x^2} - \lambda C_wA_w + E_wA_w + \alpha A_w(C_c - C_w) \quad (6)$$

$$\frac{\partial RC_iA_z\theta}{\partial t} = -\frac{\partial(u_sC_iA_z)}{\partial x} + \frac{D_s\partial^2(C_iA_z\theta)}{\partial x^2} + E_iA_z\theta \quad (7)$$

$$\frac{\partial C_cA_c}{\partial t} = \alpha A_w(C_w - C_c) - \lambda C_cA_c \quad (8)$$

where D_w is the turbulent diffusion coefficient in SW ($m^2\,s^{-1}$), D_s is the dispersion coefficient in the HZ fluid phase ($m^2\,s^{-1}$), λ is the photolysis decay coefficient (s^{-1}) and α is the CS exchange coefficient (s^{-1}). Terms $E_w = \frac{\zeta r}{Sh}$ and $E_i = -\frac{\zeta r}{Sh_s\theta}$ are related to exchanges between SW and the HZ fluid phase. Here, h_s is the depth of the HZ (m), and ζ is equal to C_i or C_w when $r > 0$ (flow calculated from Eq. (3) is directed from the HZ fluid phase to SW) or $r < 0$ (SW → HZ fluid phase), respectively. When the river widens at a given cell x_0, the CS cross-sectional area $A_c(x)$ of the following cells is given by:

$$A_c(x) = A_w(x) - A_w(x_0) \quad (9)$$

It is set to 0 in the opposite case, when the channel shrinks. Physical properties of rivers are generally width-dependent (Anderson et al., 2005). White (1993) considered that the depth of the HZ generally increases with increasing width, W, of the stream. HZ depth was consequently estimated from:

$$h_s = aW \quad (10)$$

where a is dimensionless.

Lateral inflows Q_{L_k} were calculated from Eq. (5) using GRASS 6.4 GIS. The model was numerically solved for reaches AB and BC, applying a finite-difference semi-implicit scheme for advection (Super Bee scheme) and an explicit scheme for diffusion and sink-source terms (Kampf, 2009). This was programmed in FORTRAN. Discharge at the left (upstream) boundary was maintained constant and equal to $\Sigma Q_{L_{A-1}}$, where $A-1$ is the number of cells preceding point A. An Orlansky radiation boundary condition (Herzfeld et al., 2011) was applied at the right (downstream) open boundary.

2.4. Parameter values

Table 1 lists the parameters included in the model. As suggested by Arcement (2000), Manning's roughness coefficient was calculated for reaches AB and BC, taking into account sediment classes and riverbed morphology. Previous studies in a similar headwater catchments aided in determining TOPMODEL parameters (Eq. (5)). On the basis of soil moisture surveys (Trévisan et al., 2010) and considering the tracer was injected during the dry season, a high soil saturation deficit (D) and a large decrease in hydraulic conductivity (M, Eq. (5)) were assumed. From soil granulometry analysis (Vansteelant et al., 1997) and considering pedotransfer functions (Bastet et al., 1998), hydraulic conductivity K_0 of the upper soil layer was set to relatively high values. Values of parameters involved in in-stream channel processes were calculated from previous experimental studies. We calculated the turbulent diffusion coefficient in SW from Seo and Cheong (2005):

Table 1
Model parameters. HZ: Hyporheic Zone; SW: Surface Water; CS: Channel Storage.

Parameter	Definition	Value	Source
n	Manning coefficient	0.03 (section AB) 0.08 (section BC)	Arcement (2000)
K_z	Saturated hydraulic conductivity of HZ	0.3 m s^{-1} (stones) 3×10^{-3} m s^{-1} (gravels) 4×10^{-4} m s^{-1} (fine sediment)	Holzbecher (2007)
K_0	Saturated hydraulic conductivity of saturated soil	5.5×10^{-5} m s^{-1}	Trévisan et al. (2010)
M	Decrease in K_0 with depth	0.1	Fixed
D	Soil saturation deficit	0.25	Fixed
D_w	Diffusion coefficient in SW	0.18 $m^2\,s^{-1}$ (section AB) 0.43 $m^2\,s^{-1}$ (section BC)	Calculation (Eq. (11))
λ	Photolysis decay constant	9.0×10^{-7} s^{-1}	Keefe et al. (2004)
θ	Porosity	0.25	Holzbecher (2007)
α_L	Longitudinal dispersivity	0.11	Shulze-Makuch (2005)
α	CS exchange coefficient	Table 2	Calibration
R	Retardation factor	Table 2	Calibration
a	Ratio h_s/W (Eq. (10))	Table 2	Calibration

$$D_w = hu_*5.91\left(\frac{W}{h}\right)^{0.620}\left(\frac{u}{u_*}\right)^{1.428} \quad (11)$$

where u_* is the shear velocity calculated from $u_* = \sqrt{ghS_0}$ (Martin and McCutcheon, 1998), where S_0 is the river slope.

The RWT photolysis rate coefficient λ for SW is $9.9\times10^{-8}\,s^{-1}$ (Keefe et al., 2004). Nevertheless, this number implies a half-life of about 80 days, which is significantly longer than the period simulated. Consequently, decay was ignored in calculations.

The dispersion coefficient D_s in the HZ fluid phase was determined for each cell from

$$D_s = \alpha_L u_s/\theta \quad (12)$$

where α_L is the longitudinal dispersivity. Finally, parameters a (Eq. (10)), giving the depth of the HZ and retardation factors R for bedrock/stones, riffles and pools were the only parameters obtained by calibration. This was done using a non-linear least squares algorithm in SCILAB to minimise the objective function:

$$\Sigma\left(y^{obs} - y^{calc}\right)^2 \quad (13)$$

where y^{obs} and y^{calc} are the observed and calculated values of C_w obtained simultaneously at points B and C, respectively. Calibrated parameters are presented in Table 2.

Table 2
Values of parameters a, R and α.

Reach	AB		BC	
Morphological features	Stones–bedrock	Pools	Riffles	Pools
a	0.04	0.21	0.74	1.32
R	2.51	10,792	3.64	10,792
α	1.95×10^{-8} s^{-1}			

2.5. Sensitivity analysis

Sensitivity analysis was performed to evaluate how the model responds to parameters involved in catchment hydrodynamics and river exchanges. The responses studied were the mean residence times t_j of the solute at points B and C, given by:

$$t_j = \frac{\int tC_j dt}{\int C_j dt} \quad (14)$$

where the subscript j becomes w, i or c, when SW, the HZ fluid phase and CS are considered, respectively. Following Faivre et al. (2013), we performed 500 Monte Carlo simulations to quantify the effect of model parameters. For each of them we considered random variables $Y^* \sim \mathcal{N}(\mu, \sigma = 0.1\mu)$. We performed ANOVA using JMP (SAS) to detect significant effects in model responses t_j. We tested linear responses between t_j and individual parameters, as well as interactions between parameters. The weight of significant model parameters was calculated by the ratio SSq/TSS (Sequential Sum of Squares/Total Sum of Squares).

3. Results

Discharge Q_L calculated at points B and C was 0.015 and 0.062 m^3 s^{-1}, respectively, close to values observed from sodium chloride injection (0.019 and 0.056 m^3 s^{-1}). Calculated concentrations of RWT at points B (Fig. 3) and C (Fig. 4) were similar to those observed. No bias was detected from visual inspection of residuals. The contribution of storage zones differed between bedrock and riffle-pool sections. At point B, in the bedrock section, patterns of solute concentrations in SW and the HZ fluid phase were quite similar, while the concentration in CS decreased slowly and was one-fifth of that in SW (Fig. 5). At point C, in the riffle-pool section, RWT concentrations in the HZ fluid phase and CS had similar patterns, with long tails (Fig. 6). Such patterns where also observed in previous works from BCT analysis, by a convolution between stream concentration and a transfer function associated with the residence time distribution of solutes in the river system (Gooseff et al., 2005; Haggerty et al., 2002). For bedrock and confined rivers, surface transient storage due to local long residence flow-paths are common and associated with exponential residence time distributions, while downstream, power-laws are required when a number of features contribute to making the stream water flowing into the HZ.

Sensitivity analysis showed that parameters were not correlated. The lowest correlation coefficients (0.10–0.13) were for parameters of equations governing in-stream processes. The highest correlation coefficients were for parameters describing catchment hydrodynamics, with values around 0.25 for correlation between K_0 and D or M, and 0.40 for that between D and M. These values lie below the threshold of 0.8, which is required for significance (Faivre et al., 2013). Parameters having a significant effect ($p < 0.05$) on t_w, t_i and t_c are summarised in Tables 3 and 4 for points B and C, respectively. At point B, parameters involved in catchment hydrology played a determinant role. Their contribution to the total variance in model responses (t_w, t_i, t_c) was high, especially for D, the soil moisture deficit parameter (SSq/SST = 20%), and M, the vertical distribution of moisture in soil (70%). Except for the influence of α on CS (SSq/SST = 15%), the model was not very sensitive to variations in parameters involved in in-stream processes. The main influences on river transport were Manning's coefficient (3%), HZ depth (~3%) and for the HZ fluid phase, the retardation factor in bedrock/stone situations (3%). HZ hydraulic conductivity and solute diffusion in SW had little influence. The patterns were similar at point C in downstream riffle-pool conditions (Table 4). Factors involved in catchment hydrology greatly influenced model responses. In-stream processes were controlled by both upstream and local conditions, with influence mainly from HZ geometry, followed by Manning's friction coefficient. Dynamic parameters such as HZ hydraulic conductivity and solute diffusion had little influence. Unlike for the bedrock unit, response of the CS model for the riffle-pool unit was significant but quite insensitive to variation in α (SSq/SST = 0.0004%).

4. Discussion

Several studies have been performed in headwaters to examine the fate of contaminants in bedrock, steps, riffles or pools. They provide a valuable basis for comparison and validation purposes.

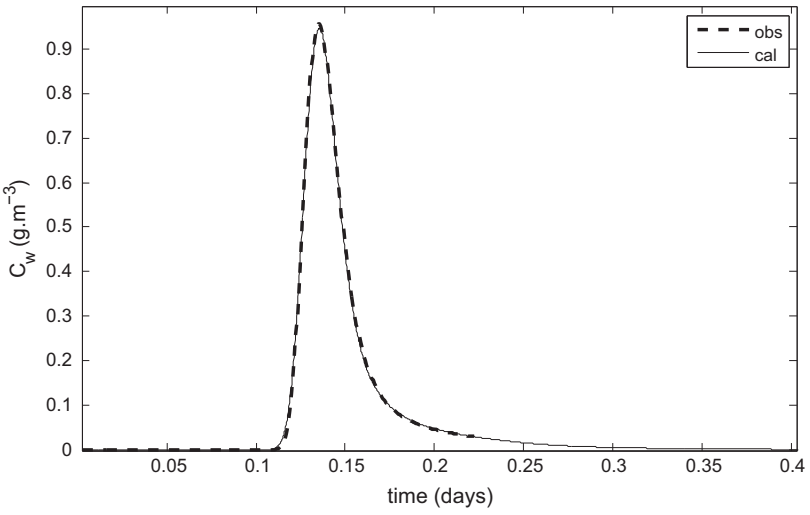

Fig. 3. Observed and calculated values of Rhodamine WT concentration at point B.

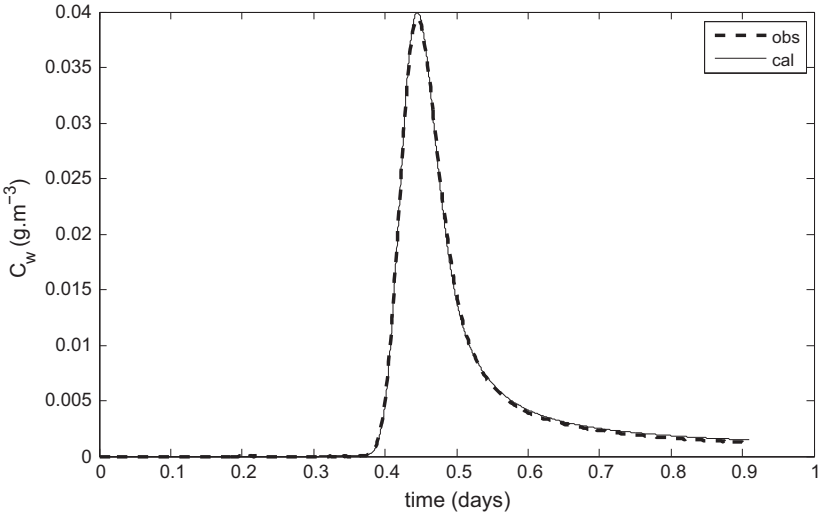

Fig. 4. Observed and calculated values of Rhodamine WT concentration at point C.

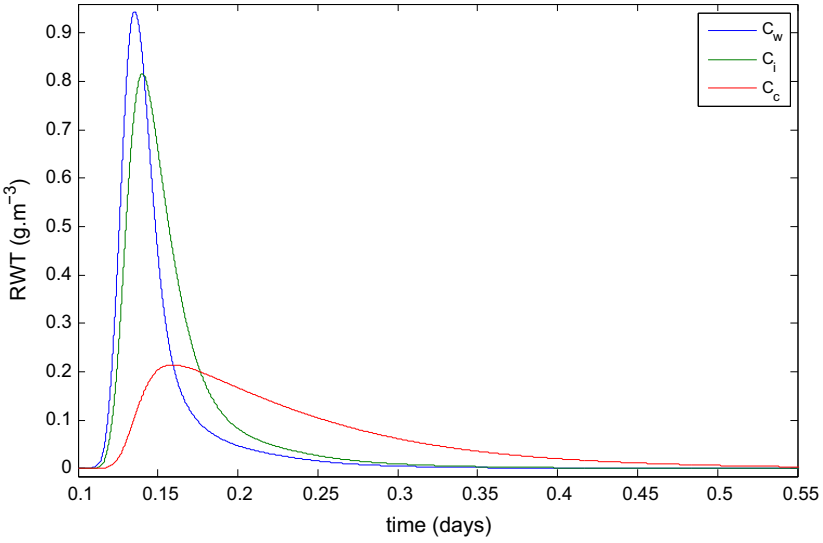

Fig. 5. Calculated values C_w of Rhodamine WT in Surface Water (SW), C_i in the Hyporheic Zone (HZ) fluid phase and C_c in Channel Storage (CS) at point B.

In field conditions, a number of studies improved the OTIS model considering two storage zones (Briggs et al., 2009; Choi et al., 2000). The MODFLOW model and the Pumping Model have been coupled to assess transient storage in various sequences of morphological features (Gooseff et al., 2006). In the laboratory, Tonina and Buffington (2007) and Cardenas and Wilson (2007) validated the linking of St. Venant's and Darcy's equations, which are commonly used to predict patterns and dynamics of HZ exchanges. These approaches constitute the basis of our study, from which a one-dimensional model combining lateral inflow and CS and HZ exchanges at a regional scale (up to 5 km long) was developed.

Given the low correlations between parameters, the latter's influences on model responses can be discussed without considering interdependency effects. Lateral inflow was calculated from TOPMODEL equations to account for the "variable source hydrology" that predominantly drives water balance in impervious hilly conditions (Trévisan et al., 2010; Easton et al., 2007). Discharges calculated by TOPMODEL were compared to measurements obtained at two sites representing the upper and lower parts of the studied river. Calculated and measured discharges were similar, but more precise for the upper part (−10% error) than for the lower part (+20% error). This is due to not having overparametrized the model, notably by defining a single set of hydraulic properties and initial soil-moisture conditions for both the upper colluvial and lower colluvial–alluvial parts of the catchment.

Due to the relatively small differences between calculated and measured discharges, calculated RWT concentrations agreed well with field data, and without bias. Calculated RWT concentration peaks closely matched those measured, but this is intrinsic to the value of Manning's coefficient, obtained from empirical tables (Arcement, 2000). Widths of BTC peaks depended mainly on the longitudinal diffusion coefficient D_w. A variety of empirical equations have been proposed to estimate D_w from several river parameters, such as the width of the wet channel, water depth, mean water velocity and bottom shear velocity (Liu, 1977; Fisher et al., 1979; Chin and Wohl, 2005; Seo and Cheong, 2005). We chose the Seo and Cheong (2005) formula as it can account for greater dispersion values when channels are sinuous, with sudden contractions, expansions or dead zones (Chin and Wohl, 2005).

Several studies have included modelling of inter-phase exchanges in natural systems. Exchanges between dissolved and solid phases have been described using Fick's law for kinetic

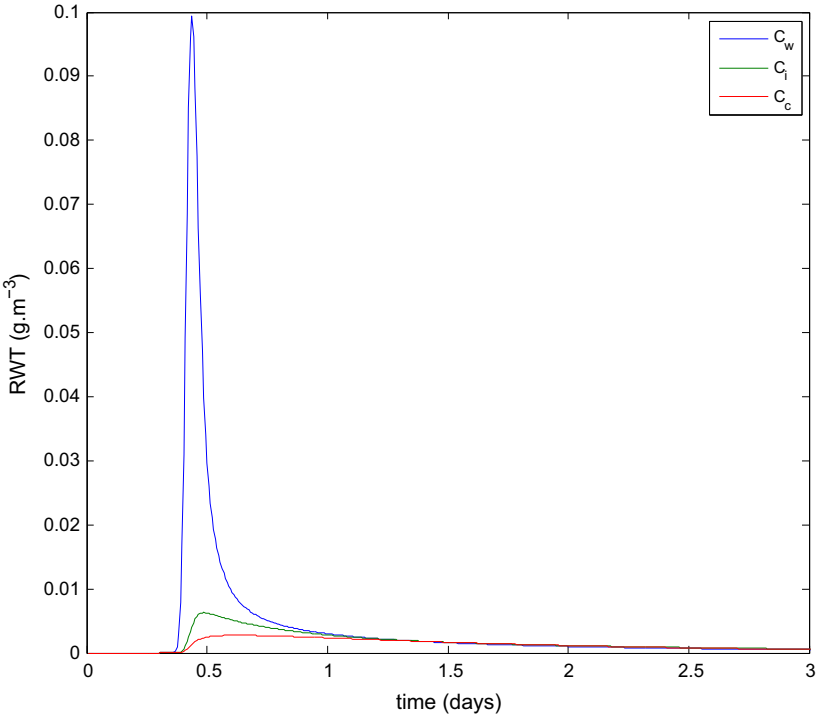

Fig. 6. Calculated values C_w of Rhodamine WT in Surface Water (SW), C_i in the Hyporheic Zone (HZ) fluid phase and C_c in Channel Storage (CS) at point C.

Table 3
Parameters having significant effects on mean Rhodamine WT residence time t_w in SW, t_i in HZ fluid phase and t_c in CS zones at point B. Parameters are defined in Tables 1 and 2; n.s.: not significant.

Parameter	t_w		t_i		t_c	
	Effect	SSq/SST (%)	Effect	SSq/SST (%)	Effect	SSq/SST (%)
n AB	+	3.1	+	2.8	+	2.3
a Stones—bedrock	+	2.7	+	3.1	+	1.4
R Stones—bedrock	+	0.6	+	3.0	+	0.9
K_z *Stones—bedrock*	n.s.	~ 0	+	0.25	n.s.	~ 0
D_w *AB*	–	0.06	–	0.04	–	0.04
α	n.s.	~ 0	n.s.	~ 0	–	15
K_0	–	1.5	–	1.5	–	1.3
D	+	20	+	19	+	17
M	–	70	–	68	–	60

Table 4
Parameters having a significant effects on Rhodamine WT mean residence time t_w in SW, t_i in HZ fluid phase and t_c in CS zones at point C. Parameters are defined in Tables 1 and 2; n.s.: not significant.

Parameter	t_w		t_i		t_c	
	Effect	SSq/SST (%)	Effect	SSq/SST (%)	Effect	SSq/SST (%)
n AB	+	0.2	+	0.2	+	0.2
n BC	+	0.09	+	0.2	+	0.09
a Stones—bedrock	+	1.2	+	1.1	+	1.1
a riffles	+	0.1	+	2.2	+	1.3
a pools	n.s.	~ 0	–	0.01	n.s.	~ 0
K_z *gravel*	+	0.7	+	0.02	+	0.2
R Stones—bedrock	+	0.07	+	0.05	+	0.06
R riffles	–	0.001	+	0.7	–	0.001
R pools	n.s.	~ 0	n.s.	~ 0	+	0.6
D_w *AB*	–	0.01	–	0.01	–	0.7
α	n.s.	~ 0	n.s.	~ 0	–	0.0004
K_0	–	1.4	–	1.4	–	1.4
D	+	20	+	20	+	20
M	–	71	–	71	–	72

transfer coefficients, along with description of the surface available for adsorption, notably the fraction of fine particles and their accessibility (Periañez, 2008, 2012). At a regional scale, where morphological features of rivers and HZ properties have high spatial variability, such description involves increasing the number of parameters and may complicate model calibration. Thus, the description of inter-phase exchanges was simplified by assuming a linear sorption isotherm and a retardation factor (Haggerty et al., 2002; Chen and Kuo, 2002), which varied along the river. As expected, RWT adsorption was negligible in the upper part of the river or in riffles: the predominance of boulders, stones or gravel is not a suitable environment for the development of adsorption sites (Periañez, 2008). Adsorption was more intense, however, in the lower step-pool unit, with a larger retardation factor, which yielded an RWT sorption isotherm $K_d = 1.3 \times 10^{-7}$ m^3 g^{-1}. This is similar to some values measured for fine sediments of mountain rivers: -5.6×10^{-6} m^3 g^{-1} (Bencala et al., 1983).

In floodplains, where surface deposits are extensive, water table levels are mainly regulated at a regional scale. This is quite different from morainic environments of mountain catchments, where interfaces between slopes and rivers consist largely of relatively small pockets of colluvial/alluvial materials (whose depths range on average from 1 to 3 m) overlying compacted and impervious layers. These materials constitute the reservoir for small localised water tables that are fed by lateral inflows from surrounding slopes (Trévisan et al., 2010). Given such geomorphological features, the expected extent of the HZ should be limited by the depth of colluvio-alluvial pockets (<2–3 m) or, in situations where erosion dominates, by a thick layer of altered substrates (<0.5 m). The HZ depth/river-width ratios calculated (Table 2) agree with the dimensions of these geomorphological features. Several authors have estimated the HZ exchange depth in modelling studies. From heat exchange measured along a first-order reach, Westhoff et al. (2011) estimated HZ depths of 0.2–0.6 m. Applying the OTIS model, Wondzell (2006) estimated HZ exchange depth to be 1.2–2.8 times

water depth in the step-pool environment. Although it is difficult to deduce the average depth of HZ exchanges from field observations in the river units studied, the calibrated ranges of HZ exchanges from our study lay in the same order of magnitude as these estimates. Using the OTIS model, Herrman et al. (2010) and O'Connor et al. (2010) estimated the cross-sectional area A_s of the storage zone (corresponding to the sum of channel and hyporheic storage) along several reaches (30–50 m long) in headwater ($A_s = 0.03 \pm 0.01\ m^2$) and riffle-pool ($A_s = 0.56 \pm 0.31\ m^2$) conditions. The values obtained are similar to those we calculated for 50-m-long sections of the studied river ($A_s = \sum_0^{50} A_c(x) + A_z(x)$): $0.015 \pm 0.002\ m^2$ and $0.66 \pm 0.31\ m^2$ for sections AB and BC, respectively.

The model includes a first order reaction rate to account for the photolysis rate of RWT. Considering the short time the RWT slug spends in the river compared to the RWT half-life in natural waters, decay processes were neglected. Due to the role of transient storage on the fate of solutes, such a simplification must be discussed by analysing the relative magnitude of the residence time of pollutants within the river system. We expect that the model is adapted to capture the effects of strong decay rates, notably photolysis effects occurring in waters exposed to long duration of sunlight, as it has been demonstrated by Keefe et al. (2004) in constructed wetlands. However, the ability of the model to integrate biological or biochemical controls on the fate of pollutants needs further work, especially to evaluate the effect of increasing the number of parameters and to asses equifinality among different parameter sets. Similarly, some assumptions are not valid or must be verified at high flow conditions. First, surface and subsurface runoff must be evaluated to calculate lateral inflow, considering a full application of TOPMODEL equations. Secondly, key parameters α (controlling CS exchanges) and a (HZ) must be strongly affected by the increase of water flow. It is known that exchanges between the main channel and embayment surface storage zone depend on channel water velocity (O'Connor et al., 2010). Considering Eq. (10), the width and HZ depth of the river increase during high flow events, but we can expect that maximum values will be reached gradually when water flow increase, implying that further RWT or solute BCT experiments must be conducted under non-steady flows to verify this assumption. The contribution of CS and the HZ to transient storage differed as a function of river morphology. The slow decrease in RWT BCT and the weight of sensitive parameters revealed that CS is the main process in the bedrock unit AB, while the HZ is the main process in the riffle-pool unit BC. In sand-bed streams, the HZ has little effect on transient storage (Stofleth et al., 2008). Our results, however, agree with similar conclusions drawn in studies by Gooseff et al. (2005) and Haggerty et al. (2002), in which HZ behaviour was controlled mainly by a succession of gravel deposits and pools. As stated by Briggs et al. (2009), rivers can display both CS and HZ exchanges and researchers have used a variety of approaches to discriminate between them. The model we developed allows the continuous recognition of CS and HZ exchanges along the river reaches, giving specific and localised information on the role of local morphologic conditions (hydrodynamic properties of surrounding soils, river bed features) on transient storage. Our model differs greatly from previous approaches based on kernel convolution (Gooseff et al., 2005; Haggerty et al., 2002) or on storage zone parametrization (Bencala and Walters, 1983; Choi et al., 2000; Chin and Wohl, 2005; Briggs et al., 2009), which are limited in their ability to quantify physical-biogeochemical interactions because variability in stream characteristics are integrated. The model allows for the coupling of predictions of transport processes and uptake rates in terms of geomorphic variables because channel form and hydraulic conditions are the engineering parameters used in stream restoration designs (Shields et al., 2003). Local recognitions of soil uses and transient storage patterns should be a prerequisite for the construction of geomorphic features such as in-channel and backwater pools (Ensign and Doyle, 2005), dams of woody material (Roberts et al., 2007), dense algal mats (Kim et al., 1992), riffle-step restoration (Kasahara and Hill, 2006).

5. Conclusion

This study combined catchment hydrology, river flow and CS and HZ exchanges at a regional scale for low-flow conditions in an upland environment. We first estimated lateral inflows feeding the river by estimating groundwater seepage from analytical equations based on catchment topography and soil properties. Lateral inflows were added to the flow balance of river cells, which was simulated using a 1D model describing hydrodynamics and exchanges with CS and the HZ. RWT was introduced as a tracer, and BTC were analysed at two points downstream to compare main river features encountered in montane basins. Model parameters were obtained mainly from databases and published literature. Parameters describing inter-phase exchange (retardation factor), HZ geometry (depth:width ratio) and the exchange coefficient with dead zones (α) were calibrated and compared with previous knowledge. RWT BCT 1 km and 4 km downstream of the injection point were reproduced well. Parameter values agree with those published.

The model shows that catchment hydrology plays a determining role in mean residence time, suggesting that terrestrial and aquatic systems should be linked more closely in simulation models. Surface CS is a major process in upstream situations where water flows over bedrock and pebbles. Downstream, where sediment deposits become frequent, HZ exchange delays also solute transfer, especially through riffle deposits with high water flow. The model we present is an attempt to better integrate physical processes to represent the fate of solutes in catchments and river networks. Compared to previous models, the two storage zone model that is well adapted to capture the nature of transient storage, our decreases the number of unknowns, avoiding the measurement of key parameters such as water flow or exchange surfaces between the main channel and CS (Briggs et al., 2009), without decreasing the accuracy of prediction. The price to pay is moreover the requirement of a precise geo-referencing of morphological features controlling CS and HZ inter-phase exchanges.

It can be used in predictive studies of stream restoration or management when detailed data of stream geometry and morphology are available.

Acknowledgments

This work was supported by funding from the Programme Explora Pro 2011 nº 11 015488 01, from the Conseil Régional Rhône-Alpes, France. We thank Ph. Quétin for his valuable assistance in the field.

References

Anderson, J.K., Wondzell, S.M., Gooseff, M.N., Haggerty, R., 2005. Patterns in stream longitudinal profiles and implications for hyporheic exchange flow at the H.J. Andrews Experimental Forest, Oregon, USA. Hydrol. Process. 19, 2931–2949.

Arcement, G.J., 2000. Guide for Selecting Manning's Roughness Coefficients for Natural Channels and Flood Plains, Technical Report WSP2339. United States Geological Survey, 67p.

Baeza, A., Garcia, E., Periañez, R., 2006. Modelling the spatio-temporal evolution of ^3H in the waters of the river Tagus. J. Environ. Radioact. 86, 367–383.

Bastet, G., Bruand, A., Quétin, P., Cousin, I., 1998. Estimation des propriétés de rétention en eau laide de fonctions de pédotransfert (FPT): une analyse bibliographique. Etude et Gestion des Sols 1, 7–28.

Bencala, K.E., Rathbun, R.E., Jackman, A.P., Kennedy, V.C., Zellweger, G.W., Avanzino, R.J., 1983. Rhodamine WT dye losses in a mountain stream environment. Water Resour. Bull. 19, 943–950.
Bencala, K.E., Walters, R., 1983. Simulation of solute transport in a mountain pool-and-riffle stream: a transient storage model. Water Resour. Res. 19, 718–724.
Beven, K.J., Kirkby, M.J., 1979. A physically based, variable contributing area model of basin hydrology. Hydrol. Sci. 24:1 (3), 47–56.
Briggs, M.A., Gooseff, M.N., Arp, C.D., Baker, M.A., 2009. A method for estimating surface transient storage parameters for streams with concurrent hyporheic storage. Water Resour. Res. 45, W00D27. http://dx.doi.org/10.1029/2008WR006959.
Buffington, J.M., Tonina, D., 2009. Hyporheic exchange in mountain rivers II: effects of channel morphology on mechanics, scales, and rates of exchange. Geogr. Compass 3/3, 1038–1062.
Cardenas, M.B., Wilson, J.L., 2007. Hydrodynamics of coupled flow above and below a sediment–water interface with triangular bedforms. Adv. Water Resour. 30, 301–313.
Chen, S.C., Kuo, J.T., 2002. Modeling the fate and transport of hydrophobic organic compounds in an unsteady river-estuarine system. Int. J. Sedim. Res. 17 (3), 197–210.
Chin, A., Wohl, E., 2005. Toward a theory for step pools in stream channels. Prog. Phys. Geogr. 29 (3), 275–296.
Choi, J., Harvey, J., Conklin, M., 2000. Characterizing multiplestreamsales of stream and storage zone interaction that affect solute fate and transport in streams. Water Resour. Res. 36, 1511–1518.
Easton, Z.M., Gérard-Marchant, P., Walter, M.T., Petrovic, A.M., Steenhuis, T.S., 2007. Hydrologic assessment of an urban variable source watershed in the northeast United States. Water Resour. Res. 43 (3), W03413. http://dx.doi.org/10.1029/2006WR005076.
Ensign, S.H., Doyle, M.W., 2005. In-channel transient storage and associated nutrient retention: evidence from experimental manipulations. Limnol. Oceanogr. 50, 1740–1751.
Environment Agency, 2009. The Hyporheic Handbook. Environment Agency E.A., 265p.
Faivre, R., Looss, B., Mahévas, S., Makowski, D., Monod, H., 2013. Analyse de sensibilité et exploration de modèles. Application aux sciences de la nature et de l'environnement.
Fisher, H.B., List, E.J., Koh, R.C., Imberger, J., Brooks, N.H., 1979. Mixing in Inland and Coastal Water. Academic press, New York.
Gerard-Marchant, P., Hively, W.D., Steenhuis, T.S., 2006. Distributed hydrological modelling of total dissolved phosphorus transport in an agricultural landscape, Part I: Distributed runoff generation. Hydrol. Earth Syst. Sci. 10, 245–261.
Gooseff, M.N., Anderson, J.K., Wondzell, S.M., LaNier, J., Haggerty, R., 2006. A modelling study of hyporheic exchange pattern and the sequence, size, and spacing of stream bedforms in mountain stream networks, Oregon, USA. Hydrol. Process. 20, 2443–2457.
Gooseff, M.N., LaNier, J., Haggerty, R., Kokkeler, K., 2005. Determining in-channel (dead zone) transient storage by comparing solute transport in a bedrock channel-alluvial channel sequence, Oregon. Water Resour. Res. 41 (6), W06014. http://dx.doi.org/10.1029/2004WR003513.
Haggerty, R., Wondzell, S.M., Johnson, M.A., 2002. Power-law residence time distribution in the hyporheic zone of a 2nd-order mountain stream. Geophys. Res. Lett. 29 (13), 18-1–18-4.
Hassan, M.A., Church, M., Lisle, T.E., Brardinoni, F., Benda, L., Gordon, E.G., 2005. Sediment transport and channel morphology of small, forested streams. J. Am. Water Resour. Assoc., 853–875
Herrman, K.S., Bouchard, V., Granata, T., Carey, A.E., Moore, R.H., 2010. The effect of riparian land use on transport hydraulics in agricultural headwater streams located in northeast Ohio, USA. Hydrol. Process. 24, 1–12.
Herzfeld, M., Schmidt, M., Griffies, S.M., Liang, Z., 2011. Realistic test cases for limited area ocean modelling. Ocean Model. 37, 1–34.
Hively, W.D., Gérard-Marchant, P., Steenhuis, T.S., 2006. Distributed hydrological modeling of total dissolved phosphorus transport in an agricultural landscape, Part II: Dissolved phosphorus transport. Hydrol. Earth Syst. Sci. 10, 263–276.
Holzbecher, E., 2007. Environmental Modeling. Springer, p. 392.
Kampf, J., 2009. Ocean Modelling for Beginners Using Open-Source Software. Springer, p. 175.
Kasahara, T., Hill, A.R., 2006. Effects of riffle-step restoration on hyporheic zone chemistry in n-rich lowland streams. Can. J. Fish. Aquat. Sci. 63, 120–133.
Keefe, S.H., Barber, L.B., Kunkel, R.L., Ryan, J.N., McKnight, D.M., Wass, R.D., 2004. Conservative and reactive solute transport in constructed wetlands. Water Resour. Res. 40 (1), W01201. http://dx.doi.org/10.1029/2003WR002130.
Kim, B.K.A., Jackman, A.P., Triska, F.J., 1992. Modeling biotic uptake by periphyton and transient hyporheic storage of nitrate in a natural stream. Water Resour. Res. 28, 2743–2752.
Liu, H., 1977. Prediction of dispersion coefficient of streams. J. Environ. Eng. Div. ASCE 103 (1), 59–69.
Martin, J.L., McCutcheon, S.C., 1998. Hydrodynamics and Transport for Water Quality Modeling. University of Georgia Ed., Athens, USA, 974p.
Neilson, B.T., Stevens, D.K., Chapra, S.C., Bandaragoda, C., 2010. Two zone transient storage modeling using temperature and solute data with multiobjective calibration: 2. Temperature and solute. Water Resour. Res. 46, W12521. http://dx.doi.org/10.1029/2009WR008759.
Obled, C., Zin, I., 2004. Topmodel: principes de fonctionnement et application. La Houille Blanche 1, 65–76.
O'Connor, B.L., Hondzo, M., Harvey, J.W., 2010. Predictive modeling of transient storage and nutrient uptake: implications for stream restoration. J. Hydraul. Eng. 136 (2), 1018–1032.
Periañez, R., 2008. A modelling study on 137Cs and 239,240Pu behaviour in the Alborán Sea, western Mediterranean. J. Environ. Radioact. 99, 694–715.
Periañez, R., 2012. Modelling the environmental behaviour of pollutants in Algeciras Bay (south Spain). Mar. Pollut. Bull. 64, 221–232.
Postma, D., Appelo, C.A.J., 2000. Reduction of Mn oxydes by ferrous iron in a flow system: column experiment and reactive transport modeling. Geochem. Cosmochem. Acta 64, 1237–1247.
Prandle, D., 1974. A numerical model of the southern north sea and river Thames. Technical Report. Institute of Oceanographic Sciences, Birkenhead, Cheshire, L43 7 RA, 80p.
Roberts, B.J., Mulholland, P.J., Houser, J.N., 2007. Effects of upland disturbance and instream restoration on hydrodynamics and ammonium uptake in headwater streams. J. North Am. Benthol. Soc. 26, 38–53.
Seo, I.W., Cheong, T.S., 2005. Predicting longitudinal dispersion coefficient in natural streams. J. Hydraul. Eng. 124 (1), 25–32.
Shields, F.D., Copeland, R.R., Klingeman, P.C., Doyle, M.W., Simon, A., 2003. Design for stream restoration. J. Hydraul. Eng. 129, 575–584.
Shulze-Makuch, D., 2005. Longitudinal dispersivity data and implications for scaling behavior. Ground Water 43 (3), 443–456.
Stewart, R.J., Wollheim, W.M., Gooseff, M.N., Briggs, M.A., Jacobs, J.M., Peterson, B.J., Hopkinson, C.S., 2011. Separation of river network-scale nitrogen removal among the main channel and two transient storage compartments. Water Resour. Res. 47 (10). http://dx.doi.org/10.1029/2010WR009896.
Stofleth, J.M., Douglas Shields, D.F., Fox, G.A., 2008. Hyporheic and total transient storage in small, sand-bed streams. Hydrol. Process. 22, 1885–1894.
Tlili, A., Dorigo, U., Montuelle, B., Margoum, C., Carluer, N., Gouy, V., Bouchez, A., Berard, A., 2008. Responses of chronically contaminated biofilms to short pulses of diuron. An experimental study simulating flooding events in a small river. Aquat. Toxicol. 87, 252–263.
Tonina, D., Buffington, J.M., 2007. Hyporheic exchange in gravel bed rivers with pool-riffle morphology: laboratory experiments and three-dimensional modeling. Water Resour. Res. 43 (1), W01421. http://dx.doi.org/10.1029/2005WR004328.
Trévisan, D., Dorioz, J.M., Poulenard, J., Quétin, P., Prigent-Combaret, C., Philippe Merot, P., 2010. Mapping of critical source areas for diffuse fecal bacterial pollution in extensively grazed watersheds. Water Res. 44, 3847–3860.
Trévisan, D., Quétin, P., Barbet, D., Dorioz, J.M., 2012. POPEYE: a river-load oriented model to evaluate the efficiency of environmental policy measures for reducing phosphorus losses. J. Hydrol., 254–266
Uijttewaal, W.S.J., Lehmann, D., van Mazijk, A., 2001. Exchange processes between a river and its groyne fields: model experiments. J. Hydraul. Eng. 127 (11), 928–936.
USAEWES, 1995. CE-QUAL-RIV1: A Dynamic, One-Dimensional (Longitudinal) Water Quality Model for Streams. Technical Report EL-95-2. USAEWES. Environmental Laboratory. Vicksburg, MS-USA, 290p.
Vansteelant, J., Trévisan, Perron, L., Dorioz, J., Roybin, D., 1997. Conditions dapparition du ruissellement dans les cultures annuelles de la rgion lémanique. Relation avec le fonctionnement des exploitations agricoles. Agronomie 17, 65–82.
Westhoff, M.C., Gooseff, M.N., Bogaard, T.A., Savenije, H.H.G., 2011. Quantifying hyporheic exchange at high spatial resolution using natural temperature variations along a first-order stream. Water Resour. Res. 47 (10), W10508. http://dx.doi.org/10.1029/2010WR009767.
White, D.S., 1993. Perspectives on defining and delineating hyporheic zones. J. North Am. Benthol. Soc. 12, 61–69.
Wondzell, S.M., 2006. Effect of morphology and discharge on hyporheic exchange flows in two small streams in the cascade Moutains of Oregon, USA. Hydrol. Process. 20, 267–387.
World Reference Base for Soil Resources, 2006. World reference base for soil resources. Technical Report. World Soil Resources Reports. Roma: FAO.
Yellow Spring Instruments, 2001. Water Tracing, In Situ Dye Fluorometry and the YSI 6130 Rhodamine WT Sensor. Technical Report. YSI Environmental – 1006 E4601, 8p.